RELAXATION AND BREAKUP OF A CYLINDRICAL LIQUID COLUMN

Mohammad Ali
Department of Mechanical Engineering
Bangladesh University of Engineering and Technology .Dhaka Bangladesh.
Akira Umemura
Department of Aerospace Engineering
Nagoya University, Furo-cho, Chikusa-ku, Nagoya 464-8603, Japan

Abstract: *Instability of capillary wave and breakup of a square cylindrical liquid column during its relaxation have been investigated numerically by simulating three-dimensional Navier-Stokes equations. For this investigation a computer code based on volume-of-fluid (VOF) method has been developed and validated with published experimental results. The result shows that the agreement of numerical simulation is quite well with the experimental data. The code is then used to study the capillary wave and breakup phenomena of the liquid column. The investigation shows the underlying physics during relaxation of the square cylindrical liquid column, illustrates the formation and propagation of capillary wave, and breakup processes. The breakup behavior for the present configuration of the liquid column shows some significant differences from those predicted by conventional jet atomization theories. The formation of capillary wave is initiated by the surface tension on the sharp edge of the square end of the cylinder and the propagation of the wave occurs due to the effect of surface tension force on the motion of the fluid. The propagation of capillary wave to the end of liquid column causes a disturbance in the system and makes the waves unstable which initiates the breakup of the liquid column. The characteristics of the capillary wave show that the amplitude of the swell grows faster than the neck of the wave and that of the tip wave grows much faster than the other waves. The velocity of the liquid particle is dominated by the pressure in the liquid column.*

Keywords*: Instability; Continuum surface force; Liquid disintegration; Capillary wave; Surface tension; VOF method*

INTRODUCTION

Liquid fuel atomization is one of the key for technological challenges in efficient mixing of fuel with oxidizer in both low and high speed transports. There are many engineering applications where the spray of liquid is used though the basic understanding of atomization is still not adequate. Efficiency of combustion systems and attendant reduction of pollutants are dependent strongly on the degree to which fuel and oxidizer are mixed before they react. No doubt, the mixing of liquid fuel depends strongly on the subsequent fuel atomization technique and the characterization of the relevant processes for its distribution in the oxidizer. Since the process of atomization is very quick and fine, a numerical simulation is performed to understand the relevant physics as well as the mechanism of atomization. Moreover the problem is of considerable fundamental interest in the fluid mechanics for a time dependent free-boundary problem and in flow-induced deformation of a variety of flexible bodies. It is also related to dispersion processes in mechanical emulsifiers.

Several methods were proposed and in use for the simulation of such flow problems. These methods are discussed in several published literatures. Gueyffier et al.[1] described a numerical scheme for interface calculations. The authors used the volume of fluid interface tracking method and a piecewise linear interface calculation in the scheme. The method of interface tracking with the connection of volume fraction and interface position was described in detail. A new model called continuum surface force (CSF) for surface tension effects on fluid motion was developed by Brackbill et al.[2]. The model interpreted the surface tension as a continuous, three-dimensional effect across an interface, rather than as a boundary value condition on the interface. Hirt et al.[3] made a short review of different methods used for embedding free boundaries and compared the relative advantages and disadvantages of these methods. The author introduced a new technique in the volume of fluid (VOF) method which worked well for complicated problems. Welch et al.[4] used a VOF based interface tracking method in conjunction with a mass transfer model and used in simulation of horizontal film boiling problem. A new algorithm for the volume tracking of interfaces in two-dimensions was proposed by Rider and Kothe[5]. The method utilized local discrete material volume and velocity data to track liquid interfaces. A Flux Line-Segment model for two-dimensional problem was employed by Ashgriz and Poo[6] for tracking the interfaces. All the above researchers used VOF method for two-phase flow problems with the conjunction of some other models and techniques. Therefore, it can be concluded that the VOF method is one of the most popular schemes for tracking interfaces and hence implemented in present algorithm.

In liquid jet atomization capillary instability and disintegration of liquid are important and interesting phenomena to the fluid dynamists. An earlier account of the work is summarized by Rayleigh[7] who performed a

delightful discussion on jet instability and published both theoretical and experimental results on capillary instability phenomena. During the contraction of liquid jet or cylindrical liquid drop the capillary waves are radiated on the fluid interfaces. These waves are caused by surface tension and generated at the tip of liquid jet. In an experiment Goedde and Yuen[8] examined the capillary instability of vertical liquid jets of different viscosities and measured the growth rates of waves for disturbances of various wavelengths. The author discussed about the drop formation and ligament detachment and showed that some non-linear effects became very pronounced especially at small wave number and dominated the growth processes. In another investigation Donnelly and Glaberson[9] performed some experiments and discussed the effects of viscosity on the capillary instability and growth rate. Also several other investigations[10~11] can be found in the literature which described general features on end pinching of elongated liquid drops, their deformation and breakup. In these investigations the authors discussed and explained the effects of initial drop shape and the relative viscosities of the two fluids on the relaxation and breakup phenomena. No capillary wave was observed at the tip of the elongated liquid drop with the conditions they considered. Obviously, the phenomenon of capillary wave is a complicated one and difficulties are there to capture this wave in the resolution.

Recently Umemura et al.[12-13] (the co-author of the present investigation) performed a series of experiments on liquid jet atomization problem and obtained a new concept on capillary instability and liquid jet breakup processes. Considering one of the jet flow conditions of Umemura et. al.[12-13], Shinjo et al.[14] performed a numerical investigation on circular liquid jet disintegration mechanism and discussed about the source of capillary instability and jet destabilization.

In present study a three-dimensional numerical code is developed and validated with experimental data. The code is then used for numerical simulation to understand the characteristics of capillary waves on the surface of the liquid column in an otherwise quiescent fluid and its breakup phenomena.

MATHEMATICAL MODELING

The flow field is governed by time dependent three-dimensional Navier-Stokes equations with surface tension force. Body forces are neglected. These equations can be expressed as

$$\frac{\partial \vec{U}}{\partial t}+\frac{\partial \vec{P}}{\partial x}+\frac{\partial \vec{Q}}{\partial y}+\frac{\partial \vec{R}}{\partial z}=\frac{\partial \vec{P}_v}{\partial x}+\frac{\partial \vec{Q}_v}{\partial y}+\frac{\partial \vec{R}_v}{\partial z}+\vec{F}_{sv} \qquad (1)$$

where,

$$U=\begin{pmatrix}\rho\\ \rho u\\ \rho v\\ \rho w\end{pmatrix},\quad P=\begin{pmatrix}\rho u\\ \rho u^2+p\\ \rho uv\\ \rho uw\end{pmatrix},\quad Q=\begin{pmatrix}\rho v\\ \rho uv\\ \rho v^2+p\\ \rho vw\end{pmatrix},\quad R=\begin{pmatrix}\rho w\\ \rho uw\\ \rho vw\\ \rho w^2+p\end{pmatrix}$$

$$P_v=\begin{pmatrix}0\\ \tau_{xx}\\ \tau_{xy}\\ \tau_{zx}\end{pmatrix},\quad Q_v=\begin{pmatrix}0\\ \tau_{xy}\\ \tau_{yy}\\ \tau_{yz}\end{pmatrix}.\quad R_v=\begin{pmatrix}0\\ \tau_{zx}\\ \tau_{yz}\\ \tau_{zz}\end{pmatrix}\quad F_{sv}=\begin{pmatrix}0\\ \sigma\kappa f n_x\\ \sigma\kappa f n_y\\ \sigma\kappa f n_z\end{pmatrix}$$

The following terms are expressed as,

$$\tau_{xx}=\lambda\left(\frac{\partial u}{\partial x}+\frac{\partial v}{\partial y}+\frac{\partial w}{\partial z}\right)+2\mu\left(\frac{\partial u}{\partial x}\right),$$

$$\tau_{yy}=\lambda\left(\frac{\partial u}{\partial x}+\frac{\partial v}{\partial y}+\frac{\partial w}{\partial z}\right)+2\mu\left(\frac{\partial v}{\partial y}\right),$$

$$\tau_{zz}=\lambda\left(\frac{\partial u}{\partial x}+\frac{\partial v}{\partial y}+\frac{\partial w}{\partial z}\right)+2\mu\left(\frac{\partial w}{\partial z}\right),$$

$$\tau_{xy}=\mu\left(\frac{\partial u}{\partial y}+\frac{\partial v}{\partial x}\right),\quad \tau_{yz}=\mu\left(\frac{\partial w}{\partial y}+\frac{\partial v}{\partial z}\right),\quad \tau_{zx}=\mu\left(\frac{\partial w}{\partial x}+\frac{\partial u}{\partial z}\right),$$

$$\lambda=-\frac{2}{3}\mu.$$

Where, u, v, w are velocities in the flow field, ρ the density, p the pressure, $\mu$the viscosity, F_{sv} the surface tension force, σ the surface tension, κ the curvature of surface, n the unit normal to the surface and f is a function for continuous change of the color variable (here density) across the thickness of fluid interface.

NUMERICAL FORMULATION

To understand the phenomena of capillary instability on the liquid surface and the disintegration processes of cylindrical liquid drop, a numerical algorithm has been developed which is used to solve time dependent three-dimensional Navier-Stokes equations with surface tension force. The algorithm can capture the capillary waves radiated on the surface of cylindrical liquid drops. For the simulation, volume-of-fluid (VOF) method with a fixed, regular, uniform grid is used to solve the problem. Piecewise Linear Interface Calculation (PLIC) is implemented for the advection of the liquid interface. The treatment of surface tension consists of artificially smoothing the discontinuity present at the interface is a Continuum Surface Force (CSF) manner[2].

RESULTS AND DISCUSSION

The present investigation can be divided into two parts: Validation of the numerical method and numerical simulation of the contraction of a square cylindrical liquid drop to understand the underlying physics for capillary wave instabilities and liquid disintegration processes. To validate the numerical method, a comparison of numerical simulation with published experimental data has been performed. Once the result of comparison is satisfied, the numerical method is applied for the rest part of investigation.

Comparison of Numerics with Experiment

The present three-dimensional numerical code is validated by comparing the simulation results with the data of Goedde and Yuen[8]. For comparison a square cylindrical water column is considered to calculate the swell and neck diameters of the capillary wave during its relaxation. The unperturbed cross sectional area of the drop and other calculation parameters such as surface tension, viscosity etc. are identical with the experiment. The time evolution of both swell and neck during numerical simulation and experiment is shown in Fig. 1. It can be pointed out that during relaxation of liquid cylinder, the capillary wave is initiated from tip of the cylinder by surface tension. Due to the shape of cylinder tip the initial growth of the first swell is rapid. Therefore, for comparison the growth of second swell is calculated which is closer to the experimental conditions from geometric point of view. As data taking manner of Goedde and Yuen[8], the growth of adjacent neck ahead of the swell is considered. For this comparison smoothed experimental data are taken from Fig. 5 of Goedde and Yuen[8]. Figure 1 shows that in general the simulation results agree quite well with the experiment. At the beginning of time evolution history very small deviation from data for both swell and neck diameter can be found. This is caused by the initial shape of the liquid column.

Figure 2 shows the re-plotting of the simulation data in Fig. 1. The Rayleigh's linearized analysis shows that the exponential growth rate is constant. Therefore, the natural logarithms of the deformations of swell, neck and the difference between the swell and neck diameter as a function of time are plotted in Fig. 2. It can be pointed out that the slopes of these curves indicate the exponential growth rate of swell and neck diameter and their differences. However, Fig. 2 shows that the exponential growth rates of swell and neck are not constant; rather the exponential growth rate of their differences is constant. The same trend of the curves was found by the experiment of Goedde and Yuen[8]. At early time the deformation of swell is slower and gradually the slope of the curve increases though the maximum part of the curve is straight. The straight part of the curve for swell has maximum slope among the curves. The minimum slope of the curve for swell is 30/sec and the maximum of that is 91/sec. The slow deformation of swell in early stage is due to the requirement of time for the propagation of surface tension force to the fluid motion. The opposite trend can be observed for the curve of neck, i.e. at early stage the deformation of neck is faster and later it becomes slower. The faster growth of neck is the consequence of the conservation of mass for the development of capillary wave. After some development of the neck, surface tension force becomes dominant due to small radius of curvature and consequently the growth of neck becomes slower. Up to the range of data plotted in Fig. 2 the maximum slope for the neck is 77/sec at the straight portion of the curve and the minimum is 34/sec. In experiment, Goedde and Yuen [8] found that the maximum slope of the curve for swell is 91/sec and that for neck is 78/sec. Also the Fig. 2 shows that though the part of the curves for both swell and neck are straight, their slopes are higher than the slope of the curve plotted for the difference between swell and neck which can be found as 72/sec. In experiment, it has been indicated as 74/sec.

From the above comparison excellent agreement of the present numerics with the experimental data can be found. With the level of accuracy indicated by this comparison and discussion it can be concluded that the present numerical method is capable of capturing the capillary

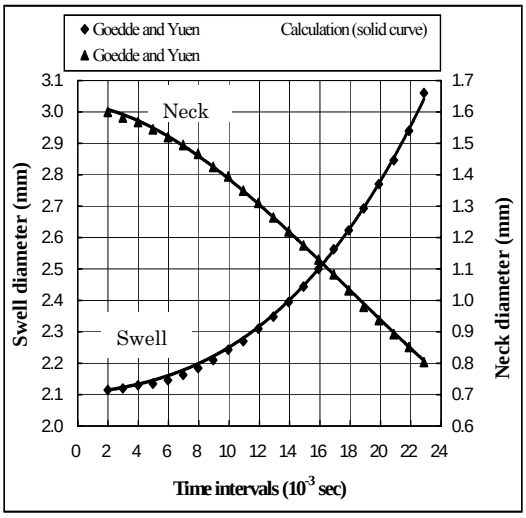

Fig.1: Comparison of swell and neck diameters with experiment; Average diameter of unperturbed cylinder, D_0 = 1.86 mm

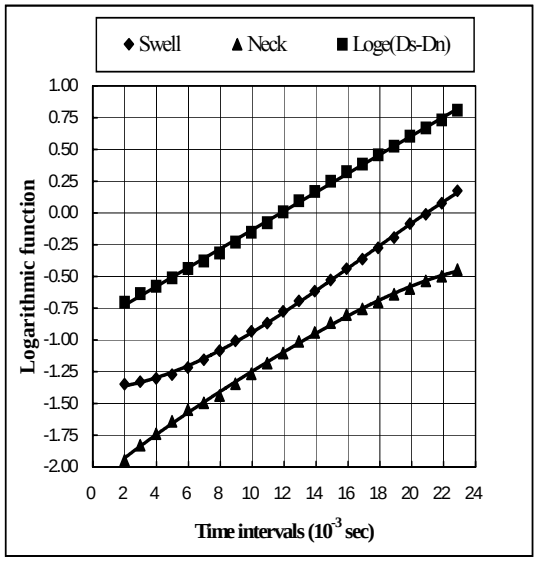

Fig.2: Logarithmic plot of calculation in Fig. 1 as a function of time. Ds denotes diameter of swell and Dn diameter of neck. Symbol ◆ is for $\log_e[Ds(t)-D_0]$; ▲ for $\log_e[D_0-Dn(t)]$; ■ for $\log_e[Ds(t)-Dn(t)]$. The curve of $\log_e[D_0-Dn(t)]$ has been shifted downward by a scale reading of 0.5.

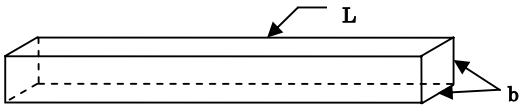

Fig.3: Schematic of the undisturbed cylindrical liquid drop.

wave and can be a tool to investigate the phenomena of capillary instabilities. Therefore, the numerical method is then used to examine the detailed dynamics of a square cylindrical liquid column during its relaxation process.

Problem Statement and Boundary Conditions

The present three-dimensional numerical scheme is used to simulate the contraction of a square cylindrical liquid drop in an otherwise quiescent gas as well as the capillary waves formed on the liquid gas interfaces. The schematic of the undisturbed cylindrical liquid drop is shown in Fig. 3. The width of the cylinder, "b" is 2.2×10^{-4} m and the cylinder half length and width ratio, L/b is 17.32. For convenient expression and easy understanding the average radius of the cylinder is calculated as the square root of (cross sectional area/π) and denoted as "a". The average diameter "d" is then calculated as d=2a. Therefore, the ratio of half length and average radius, L/a is 30.73. Sulfur hexafluoride (SF_6) of critical temperature, 318.7 K and critical pressure, 3.76 MPa is used as liquid. Gaseous nitrogen is used as immiscible, viscous fluid with pressure of 7.0 MPa. The above numerical parameters are used for this calculation as the co-author[12~13] of this paper has conducted a series of experiments on atomization problem using the same parameters and published important results.

The rectangular coordinate system has been considered for this calculation. The grids are cubic and uniform in the whole calculation domain. The width of calculation domain is eight times larger than the half width of liquid column. As the liquid column contracts, only a few grid points have been considered beyond the shrinkage end of the column. The other end of the column coincides with the domain boundary on which symmetric boundary conditions are imposed. Therefore contraction of liquid column is observed from only one end. Solid boundary conditions are imposed on other boundaries of the calculation domain.

Capillary wave and drop formation

The time evolution history of capillary wave and droplet formation during the contraction of liquid cylinder is shown in Fig. 4. The dimensionless time reported here has been calculated as the ratio of real time and the timescale,

$$t_c = \sqrt{\frac{\rho_l a^3}{\sigma}},$$

where ρ_l is the density of liquid, a the average radius of the liquid cylinder and σ, the surface tension. Here the dimensionless time is denoted by "t". Initially the tip of the liquid cylinder is rectangular in shape. The surface tension force at the sharp edge of the liquid cylinder tip initiates the formation of capillary wave. Due to surface tension the cubic end of liquid cylinder changes gradually and forms capillary wave and a bulbous end. From the beginning of calculation the formation of capillary wave starts and a complete wave including swell and neck forms at about dimensionless time, t=1.4. The wave then propagates and generates second wave at time, t=2.82. The propagation time for second wave is shorter than that for third, fourth and fifth wave. The time interval for third, fourth and fifth wave is almost same after generation of second wave and it is equal to the dimensionless time of 4.23. This uneven time interval for wave propagation is caused by the surface tension force at the end of liquid cylinder. The amplitude of the first wave (tip wave) gradually becomes larger and forms a droplet at t=18.2. It has been observed that the growth of swell and neck of the droplet is not uniform. An exponential growth of both swell and neck can be found during the relaxation process of the liquid cylinder. However by a close observation it has been revealed that the breakup does not occur unless and until the capillary wave reaches to the symmetric end of the liquid cylinder. The arrival of capillary wave to the end of the column causes a disturbance in the process and makes the capillary wave unstable and eventually breakup occurs. This instability of the wave can be understood by rapid changes of the amplitudes as shown in Fig. 4. The diameter of the first droplet is 2.12 times larger than the average diameter of the liquid cylinder. First three waves from tip wave are considered to observe the instability and the variation of amplitude. Here the amplitude is denoted as "A" measured from undisturbed surface formed by average diameter of the cylindrical liquid column and is considered as positive for swell and negative for neck. The amplitude is made dimensionless by average radius of the liquid cylinder. The capillary wave initiated from the tip of cylinder reaches to the symmetric end of the cylinder at t=15.4. Instability occurs after this time and therefore, to observe the instability the amplitudes from time 9.0 are plotted in Fig. 5. It can be observed that the amplitude of the first swell is always much larger than that of the following swells of the waves which is caused by the effect of liquid column shape at the end. We can see that after time, t=16.0 the amplitudes of both swell and neck of all waves grow faster than previous. The neck of the first wave which is the farthest away from symmetric end of the liquid cylinder grows much faster and makes a droplet at time, t=18.2. The amplitudes of waves in longer distance grow faster than that in shorter distance which is the characteristics of the unstable waves. It can also be observed that before time, t=16.0 the growing rate of first swell (tip wave) becomes lower which indicates that the pinching process is just lapsing time for unstable waves. Once the system becomes unstable, the instability of the waves expedites the liquid breakup process. This self-excitation of the instability is different from conventional jet instability theory. A more detailed discussion about the self-sustained instability mechanism can also be found in Umemura et al.[12~13].

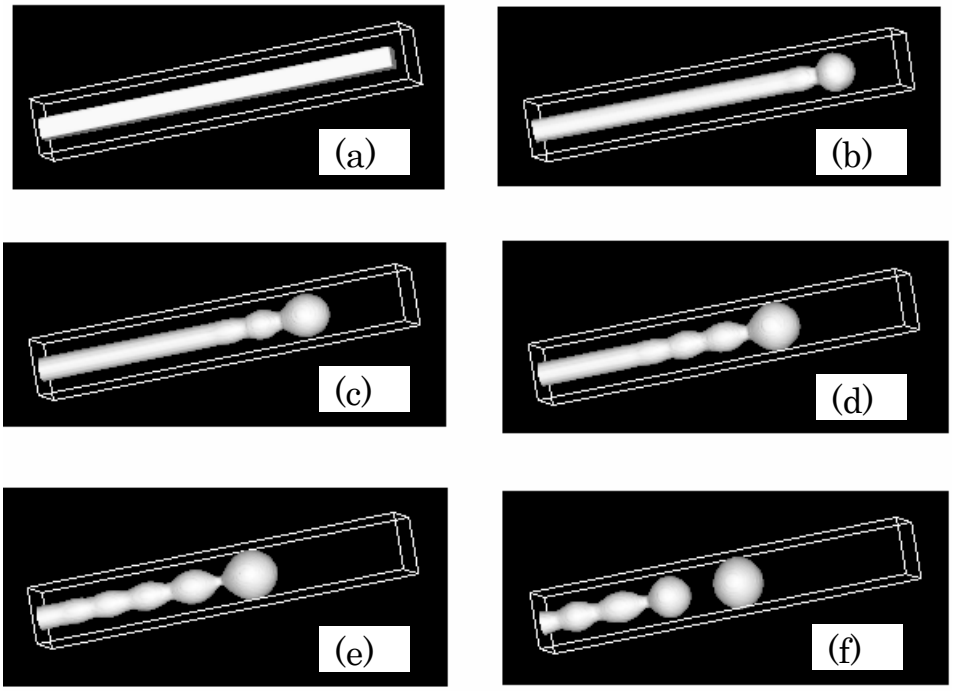

Fig. 4: Evolution of capillary wave and liquid disintegration; (a) At dimensionless time, t=0.0, (b) t=4.2, (c) t=8.4, (d) t=12.6, (e) t=16.8 (f) t= 21.0

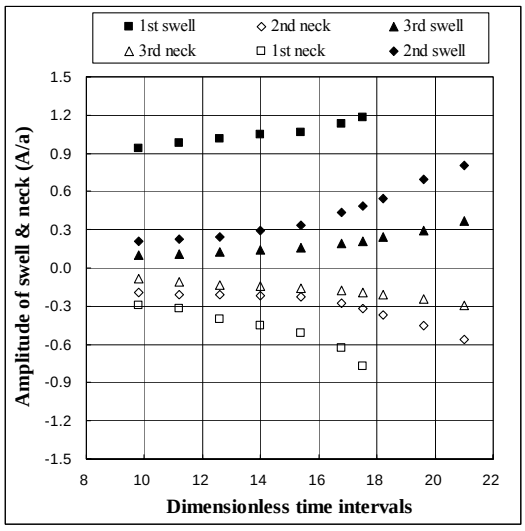

Fig.5: Variation of wave amplitudes with different time intervals.

Characteristics of capillary wave

Figure 6 shows the evolution of wave profiles with time for the first three waves. The profiles of different waves are drawn on the basis of their propagation time. The evolution time of different wave profiles is counted from the trace out moment of that wave. The wave profiles are observed at time t=4.1~14.1 with equal time interval between the adjacent profile to study the shape of the wave at different times and the growth of swell and neck. The height of wave profile denoted by A_x at different position along the wave length is normalized by average radius of the liquid column. To plot the profiles, only half of the wave length is considered. Though the wave lengths of various waves are not equal, the distance along the wave length is normalized by the half wave length to make it unity. From Fig. 6 we can see that for all waves the span of swell is broad and that of the neck is narrow, and for first wave (tip wave) the span of the swell is much broader than the other waves.

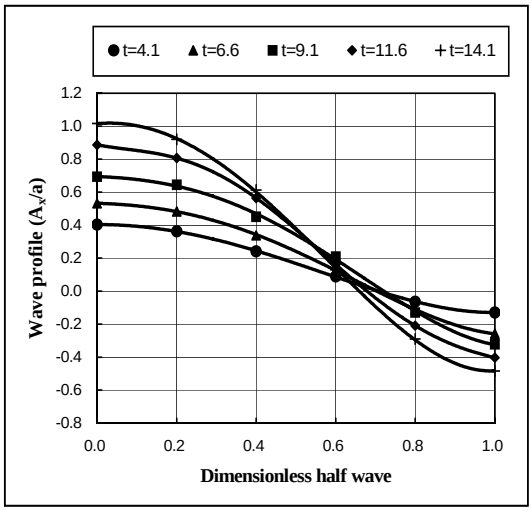

Fig. 6(a): Profiles of first wave (tip wave).

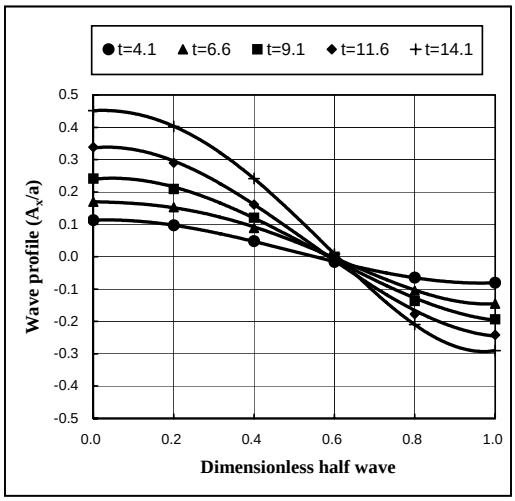

Fig. 6(b): Profiles of second wave.

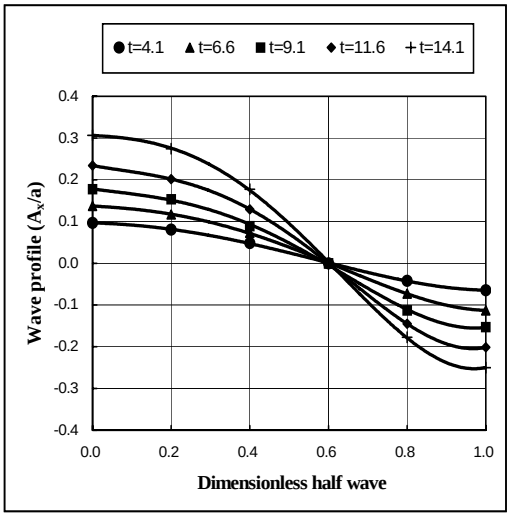

Fig. 6(c): Profiles of third wave.

Fig. 6: Variation of wave profiles with different times.

Figure 6(a) shows that though initially the span of neck is about one third of the swell, with time being the span of neck broadens narrowing the span of the swell. For second and third waves as shown in Figs. 6(b) and (c) we can see that the neck broadens with nodal point moving inward of the swell. During the evolution the nodal point for second wave remains fixed near the distance 3/5 of the wave length from swell side and for third wave the nodal point is very clear which moves more inward of the swell and remains fixed exactly at distance 3/5 of the wave length from swell side. In general the swell grows faster than the neck and for the swell the growing rate increases with time except for the wave profile at time t=14.1 of the first wave as shown in Fig. 6(a). It has been observed that the growing rate of the first swell is low at around time t=14.1 while the capillary wave tends to reach the symmetric end of the liquid column before initiating the capillary wave unstable as discussed earlier. Another observation is that the amplitude of the first wave is always much higher than that of the other waves which is caused by the surface tension force at the contraction end of liquid column. Gradually the amplitude decreases for the later waves, which is caused by the effect of viscosity.

Figure 7 shows the variation of pressure along the horizontal axis of liquid cylinder at time t=14.1 when few capillary waves have already been formed. The pressure on the central axis at different position of capillary waves can be understood from this figure. In fact the surface tension force causes pressure variation in the liquid and eventually produces fluid motion and capillary waves.

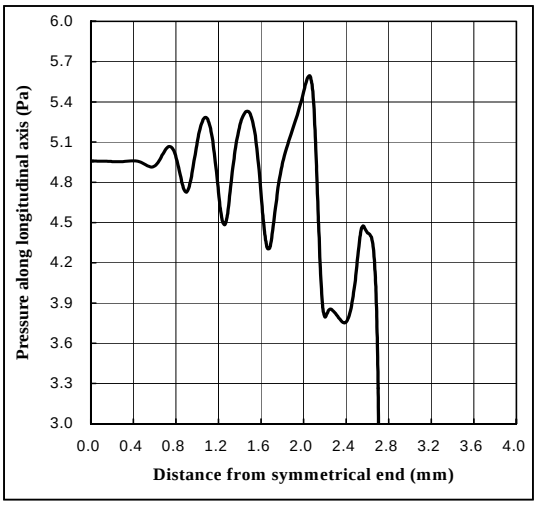

Fig. 7: Variation of pressure along the longitudinal axis of liquid cylinder.

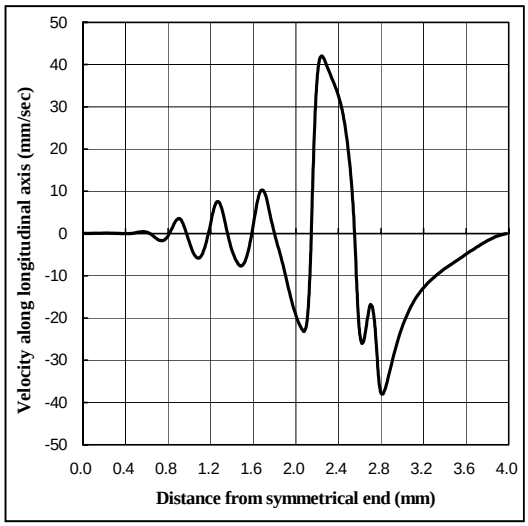

Fig. 8: Horizontal velocity profile along the longitudinal axis of liquid cylinder.

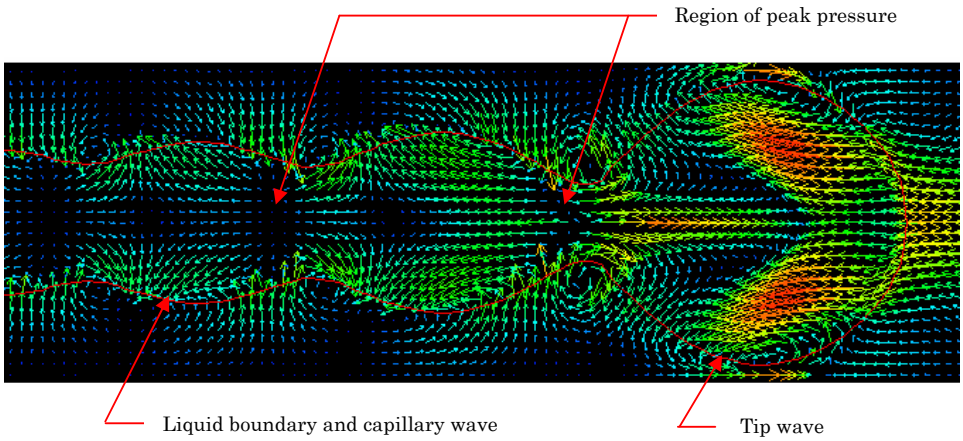

Fig. 8 A part of velocity vector plane through longitudinal axis of liquid cylinder.

For easy understanding about the variation of pressure and its effect on the motion of the fluid, the velocity along the axis of the liquid column and the velocity vector at the mid-plane are drawn in Figs. 8 and 9, respectively. Figure 7 shows the pressure of liquid taking the gas pressure as reference. No doubt the liquid pressure is always higher than the gas pressure and the pressure varies within the liquid depending on the surface tension force and fluid motion. Due to variation of pressure, motion of the fluid occurs and accordingly from Figs. 7 and 8 we can see that at the position of peak pressure the motion of fluid is almost zero, from this position of peak pressure motion of fluid starts towards opposite direction and horizontal velocity attains peak value towards both right and left of the peak pressure as shown in Fig. 8. It can be pointed out that the maximum pressure in liquid occurs at immediate behind (left side) of the first neck and the bulbous region has the lowest pressure. After the bulbous region several peak values on both high pressure and low pressure sides can be found in Fig. 7. The peak value of pressure is caused by surface tension and fluid motion. The overall fluid motion can be understood from Fig. 9 which shows a part of velocity vector plane of the fluid through horizontal axis of the liquid cylinder. Both vector length and color represent the magnitude of the velocity. The red color indicates the maximum velocity which is equal to 48 mm/sec. From this figure we can see that at the trough of every neck there is a vortex. The inertia force of the fluid motion in vortex increases the pressure with surface tension force at immediate behind of the trough of the neck. The inertia force of the fluid motion in same vortex as shown in Fig. 9 works towards outward direction of the cylinder at immediate right side of the trough of the neck and decreases the pressure and eventually causes the lowest peak pressure as shown in Fig. 7. The peak value of both high and low pressure gradually decreases with the decrease of wave amplitudes for both swells and necks. The decrease of peak pressure is the consequences of increase in radius of curvature and decrease in the fluid motion as can be found in Fig. 9. Similarly the peak values of horizontal velocity towards both positive and negative directions decrease with the decrease of amplitudes which decreases the narrowness of the neck and width of the swell. The decrease of horizontal velocity is the consequences of conservation of mass.

CONCLUSIONS

A numerical method has been developed to study the relaxation and breakup phenomena of a cylindrical liquid column by simulating three-dimensional Navier-Stokes equations. Excellent agreement of numerical simulation can be found with the experimental results of Goedde and Yuen[8]. The capillary instability and breakup characteristics are studied during relaxation of a square cylindrical liquid column. Calculation shows that capillary wave generates from the tip of liquid cylinder due to the effect of surface tension force and evolution of the tip wave depends on the shape of the cylinder tip. From the initial stage the swell-growth of the first wave (tip wave) is much higher than that of later waves which is caused by the surface tension force on the shape of the liquid cylinder tip. The propagation of capillary waves to the symmetrical end of the cylindrical liquid column causes a disturbance on the system and makes the relaxation process unstable. Due to instability of the process the amplitudes of both swell and neck grow rapidly and eventually pinch-off occurs. Wave profiles show that in general the span of neck from nodal point is shorter than that of swell and the span of first neck is much shorter than that of the other necks. It is found that at early stage the neck grows faster than the swell and later the reversed trend can be found. The faster grow of neck is caused by the consequences of the conservation of mass. Depending on the motion of fluid and surface tension, pressure along the longitudinal axis of liquid cylinder fluctuates and peak values of both low and high pressure sides decrease with the decrease of amplitudes of both swell and neck.

REFERENCES

[1] Gueyffier, D., Li, J., Nadim, A., Scardovelli, R. and Zaleski, S., "Volume-of-Fluid Interface Tracking with Smoothed Surface Stress Methods for Three-Dimensional Flows", J. Computational Physics, 152, pp. 423-456, 1999.

[2] Brackbill, J. U. Kothe, D. B. and Zemach, C., "A Continuum Method for Modeling Surface Tension", J. Computational Physics, 100, pp. 335-354, 1991.

[3] Hirt, C. W. and Nichols, B. D., "Volume of Fluid (VOF) Method for the Dynamics of Free Boundaries", J. Computational Physics, 39, pp. 201-225, 1981.

[4] Welch, S. W. J. and Wilson, J., "A Volume of Fluid Based Method for Fluid Flows with Phase Change", J. Computational Physics, 160, pp. 662-682, 2000.

[5] Rider, J. W. and Kothe, " Reconstructing Volume Tracking", J. Computational Physics, 141, pp. 112-152, 1998.

[6] Ashgriz, N. and Poo, J. Y., "FLAIR: Flux Line-Segment Model for Advection and Interface Reconstruction", J. Computational Physics, 93, pp. 449-468, 1991.

[7] Rayleigh, L., "On the Capillary Phenomena of Jets", Proceedings of the Royal Society of London, Vol. 29, pp. 71-97, 1879.

[8] Goedde, E. F. and Yuen, M. C., "Experiments on Liquid Jet Instability", J. Fluid Mech., Vol. 40, part 3, pp. 495-511, 1970.

[9] Donnelly, R. J. and Glaberson, W., "Experiments on the Capillary instability of a liquid Jet", Proceedings of the Royal Society of London, Series A, Vol. 290, pp. 547-556, 1966.

[10] Stone, H. A., Bently, B. J. and Leal, L. G., "An Experimental Study of Transient Effects in the Breakup of Viscous Drop", J. Fluid Mech, 173, pp. 131-158,1986.

[11] Stone, H. A. and Leal, L. G., "Relaxation and Breakup of an Initially Extended Drop in an Otherwise Quiescent Fluid", J. Fluid Mech, 198, pp. 399-427, 1989.

[12] Umemura, A., "Micro-gravity Study on Instability of Near Critical Mixing Surface jet (Mechanisms of Rayleigh-Taylor Instability Excitation at Nozzle Exit and Short Spacing Disintegration", J. Combustion Society of Japan, 46, 135, pp. 50-59, 2004 (in Japanese).

[13] Umemura, A. and Wakashima, Y., "Atomization Regimes of a Round Liquid Jet with Near-Critical Mixing Surface at High Pressure", Proceedings of the Combustion Institute, 29, pp. 633-640, 2002.

[14] Shinjo, J., Ogawa, S and Umemura, A., "Numerical Simulation of Circular Liquid Jet Disintegration due to Capillary Force", Proceedings of the Sixth Asia-Pacific Conference on Combustion, Nagoya, Japan, 20-23 May 2007, pp. 623-626.